ELSEVIER

S0032-3861(96)00891-9

Polymer Vol. 38 No. 13, pp. 3359–3367, 1997

0032-3861/97/$17.00 + 0.00

Poly(*p*-iodophenylacetylene): synthesis, characterization, polymer stability and photoelectrical properties

J. Vohlídal*, J. Sedláček and M. Pacovská
Department of Physical and Macromolecular Chemistry, Faculty of Science, Charles University, Albertov 2030, CZ-128 40 Prague 2, Czech Republic

and O. Lavastre and P. H. Dixneuf
Laboratoire de Chimie de Coordination et Catalyse, URA CNRS 415, Campus de Beaulieu, Université Rennes 1, F-35042 Rennes, France

and H. Balcar
J. Heyrovský Institute of Physical Chemistry, Academy of Sciences of the Czech Republic, Dolejškova 3, CZ-182 00 Prague 8, Czech Republic

and J. Pfleger
Institute of Macromolecular Chemistry, Academy of Sciences of the Czech Republic, Heyrovský Sq. 2, CZ-162 06 Prague 6, Czech Republic
(Received 26 June 1996; revised 17 September 1996)

New functional acetylene, 1-ethynyl-4-iodobenzene, (*p*-iodophenylacetylene) was prepared, characterized (i.r., n.m.r., u.v. and mass spectra) and transformed into high-molecular-weight polymers. Various $WOCl_4$-based and $MoCl_5$-based catalysts were used in the polymerization, the former leading to the red soluble and the latter to dark red insoluble poly(*p*-iodophenylacetylene) (PIPA), respectively. Both types of PIPA are non-crystalline and they differ in the configurational structure which, however, could not be assigned with certainty. A too high molecular weight and/or cross-linking is suggested as a reason of insolubility of PIPA prepared on Mo-based catalysts. The soluble PIPA was found to degrade autoxidatively in tetrahydrofuran solution at room temperature obeying the kinetic laws of polymer random degradation. The determined value of the rate constant of degradation, $2.6 \times 10^{-6}\ min^{-1}$, is slightly higher than that found for unsubstituted poly(phenylacetylene) (PPA), under the same conditions. PIPA was found to possess a higher photoconductivity than PPA at low and moderate electric fields. The Onsager model offers an adequate explanation for the measured dependence of the photogeneration efficiency of the applied electric field assuming the Gaussian distribution of the radii of charge-transfer states. © 1997 Elsevier Science Ltd.

(Keywords: *p*-iodophenylacetylene; metathesis polymerization; conjugated polymers)

INTRODUCTION

Polymers of substituted acetylenes are virtual insulators. However, those mainly bearing aromatic pendant groups can capture, transport and mediate mutual conversions of charge and energy[1–7]. In addition, some of them exhibit non-linear optical properties[2–5,8–11]. These polymers are therefore studied as potential active materials for functional elements in information technologies although they are often unstable in air[1,7,8] particularly in solutions[12–15].

Various polyacetylenes with aromatic and related pendant groups have been prepared (for general survey, see refs 2, 4, 6 and 7) and studied as to their electrochromism, photoconductivity and related properties[16–27], such as PPA and its various ring substituted derivatives (alkyl, alkoxy, bromo, chloro, $-CF_3$, $-Si(CH_3)_3$, *o*-phenyl), poly[(N-carbazolylmethyl)acetylene], poly[(N-phenothiazinylmethyl)acetylene] and some copolymers of these monomers. In addition, other polyacetylenes involving conjugated substituents have been prepared including those containing metals, e.g. ferrocenyl, ruthenocenyl[28,29], and zwitterions[26,30]. However, to our knowledge, no iodo-substituted poly(phenylacetylene) has been reported in the literature. Probably the only reported polymer of iodo derivative of acetylene is poly(diiodoacetylene)[31]. It is well known that iodine is often used for doping polyacetylenes to increase their conductivity and that this doping is accompanied by a partial iodination of the polymer main chain[1–5] deteriorating electrical properties of the polymer. In the case of iodination of side groups, no dramatic change in the electrical conductivity can be expected. However, the iodine substituent (as an electron acceptor) attached to a conjugated side group linked with the conjugated main chain can play a substantial role in the overall process

* To whom correspondence should be addressed

of the free charge carrier photogeneration due to both electronic and steric effects.

In the present paper we report on the preparation, stability (degradability) and physicochemical and photoelectrical properties of the hitherto unreported polymers of *p*-iodophenylacetylene in native state.

EXPERIMENTAL

Materials

Solvents used in the *p*-iodophenylacetylene synthesis were of analytical or reagent grade and they were dried by standard methods. 4-(Trimethylsilylethynyl)aniline, compound **A**, was prepared by the procedure described previously[32]. Benzene (Lachema, Czech Republic), 1,4-dioxane (Lachema), $WOCl_4$ (Aldrich) and $(C_6H_5)_4Sn$ (Aldrich) were purified as described earlier[13,14]. $MoCl_5$ (Aldrich) and $(C_4H_9)_4Sn$ (Aldrich) were used as supplied. Tetrahydrofuran (THF) (Aldrich, purity 99.5%+, stabilized with 2,6-di-*tert*-butyl-*p*-methylphenol, 0.025% w/v) was used as an eluent in size exclusion chromatography (s.e.c.) and solvent in degradation experiments. Poly(phenylacetylene) used as a material to which the results of photoelectrical measurements on PIPA were compared was prepared with $WOCl_4/2$ Ph_4Sn catalyst in the benzene/dioxane (1/1 by volume) mixed solvent. The details of procedure are described elsewhere[14].

Methods of monomer and polymer characterization

Elemental analyses were performed by the CNRS analysis laboratory, Villeurbanne, France.

N.m.r. spectra were recorded in $CDCl_3$ solutions using the following instruments: (a) Bruker AC 300 P operating at 300.13 MHz for ^1H and 75.47 MHz for ^{13}C; (b) Varian Unity 200 operating at 200.06 MHz for ^1H and 64.16 MHz for ^{13}C; and (c) Bruker AM 200 MAS operating at 64.16 MHz for ^{13}C.

Mass spectra were obtained on a high-resolution mass spectrometer Jeol MSD 100 operating in EI mode. Samples were introduced via a direct inlet and evaporated from a capillary nozzle (inside diameter 0.1 mm) at 40 and 60°C.

G.c.-m.s. analyses of supernatants from isolation of polymers were carried out on a Hewlett-Packard 5890 (Series II) instrument with a HP 5971A MSD detector using a SPB-1 capillary column (length 30 m, inner diameter 0.2 mm), injector temperature 250°C, programmed temperature from 65 to 275°C (5°C min^{-1}).

I.r. spectra were recorded using an ATI Matson Genesis Series *FT*i.r. spectrometer and the diffuse reflectance technique (non-diluted powdered samples, 128 scans at resolution 4 cm^{-1}).

U.v./vis optical absorption spectra were recorded on a Hewlett–Packard 8452 diode-array spectrometer using quartz cuvettes (0.2 cm) and freshly distilled THF as a solvent.

Size exclusion chromatography (s.e.c.) analyses were made on a TSP (Thermo Separation Products, Florida, USA) chromatograph fitted with u.v. detector operating at 254 nm. A series of two PL-gel columns (Mixbed B and Mixbed-C, Polymer Laboratories Bristol, UK) and stabilized THF (flow rate 0.7 ml min^{-1}) were used. Molecular weight averages relative to polystyrene standards are reported.

Procedures

Preparation of 1-iodo-4-(trimethylsilylethynyl)benzene, **B**. A slight stoichiometric excess of sodium nitrite (3.25 g, 47 mmol) dissolved in water (25 ml) was added to a slurry of amino compound **A** (8.50 g, 45 mmol) in concentrated hydrochloric acid (25 ml) at 0°C. An orange mixture formed within 45 min was added dropwise into a solution of potassium iodide (9.68 g, 58 mmol) in water (450 ml) at 0°C. The resulting mixture was allowed to reach the room temperature and stirred overnight. The crude product was extracted from water phase with diethyl ether in three steps (400 ml and twice 60 ml). The combined organic layers were washed with brine and dried with magnesium sulfate. After evaporation of the solvent, the brown crude product was purified by column chromatography on alumina using pentane as an eluent to give 8.34 g of white solid (yield 62%).

Characterization of **B**. *I.r.*: 2157(*m*) cm^{-1} $\nu(C{\equiv}C)$. ^1H *n.m.r.* (300.131 MHz, $CDCl_3$, 297 K) δ in ppm: 7.44*d* (2, H2, $J_{H-H} = 8.4$ *Hz*); 6.99*d* (2, H3, $J_{H-H} = 8.4$ *Hz*); 0.05*s* (9, H7). $^{13}C\{^dH\}$ *n.m.r.* (75.469 MHz, $CDCl_3$, 297 K) δ in ppm: 137.41 (2, C2), 133.47 (2, C3), 122.69 (C4), 104.02 (C6), 95.94 (C5), 94.48 (C1), −0.08 (3, C7). *Elemental analysis:* calculated for $C_{11}H_{13}ISi$ (found) C: 44.01 (44.65), H: 4.36 (4.56).

Synthesis of 1-iodo-4-ethynylbenzene, **C** *(*p*-iodophenylacetylene)*. An equimolar amount of aqueous sodium hydroxide (1 M solution) was added to a stirred solution of **B** (1.5 g, 5 mmol) in the mixture of methanol (10 ml) and THF (10 ml). After 30 min the solvents were removed under reduced pressure (10 mmHg). The residue was extracted with 50 ml of diethyl ether and the organic layer dried with magnesium sulfate. The crude product (yield 95%) obtained after the solvent evaporation was purified by column chromatography on alumina with pentane as an eluent to give 0.72 g of white crystalline product (63% yield).

Characterization of **C**. *I.r.* (see *Figure 1*): 3268(*s*) cm^{-1} $\nu(\equiv C-H)$; 2103(*w*) cm^{-1} $\nu(C{\equiv}C)$. ^1H *n.m.r.* (300.131 MHz, $CDCl_3$, 297 K), δ in ppm: 7.54*d* (2, H2, $J_{H-H} = 8$ Hz); 7.12d (2, H3, $J_{H-H} = 8$ Hz); 3.01(*s*) (1, H6). $^{13}C\{^dH\}$ *n.m.r.* (75.47 MHz, $CDCl_3$, 297 K), δ in ppm: 137.53 (2, C2), 133.62 (2, C3); 121.64 (C4); 94.49 (C1), 82.72 (C5) and 78.61 (C6). *Elemental analysis:* calculated for C_8H_5I (found) C: 42.12 (42.79), H: 2.21 (2.26). *Mass spectrum* *m/z* (assignment) (relative intensity): 228 (M^+) (100); 127 (I^+) (2); 114(M^{2+}) (7.5); 101 (M^+-I) (66.5); other fragments *m/z* (relative intensity): 98 (3); 75 (27); 74 (12); 62 (3); 51 (13); 50 (8). *U.v./vis:* 256 nm. $\varepsilon_{256} = 6 \times 10^4$ mol^{-1} dm^3 cm^{-1} (see *Figure 2*).

Polymerization of **C**. The standard vacuum break-seal technique was applied in all polymerization experiments, conditions: [catalyst] = 3.3 mmol l^{-1}, [monomer] = 170 mmol l^{-1}, benzene as a solvent, reaction time 24 h, room temperature. Polymerizations

Table 1 Survey of polymerization experiments; conditions: [catalyst] = 3.3 mmol l^{-1}; [monomer] = 0.17 mol l^{-1}, polymerization time 24 h, room temperature, benzene; $\langle M\rangle_w$ is weight-average and $\langle M\rangle_n$ number-average molecular weight of the polymer

Catalyst	Monomer conversion (%)	Polymer yield (%)	$10^{-3}\langle M\rangle_w$	$10^{-3}\langle M\rangle_n$	$\langle M\rangle_w/\langle M\rangle_n$
1 $MoCl_5$	96	25		Insoluble	
2 $MoCl_5$/*n*-Bu_4Sn	82	19		Insoluble	
3 $MoCl_5/Ph_4Sn$	95	10		Insoluble	
4 $WOCl_4$	90	75	53	19	2.77
5 $WOCl_4/2Ph_4Sn$	97	53	36	12	3.0
6 $WOCl_4/2Ph_4Sn$/Diox[a]	>99	90			
6a soluble in react. mixt.		20	44	26	1.71
6b insoluble in react. mixt.		70	190	110	1.74

[a] Polymerization in benzene/dioxane (1 : 1, vol.)

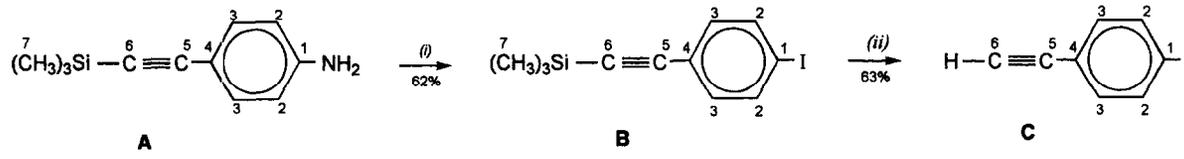

Legend: *(i)* HCl (12 M), $NaNO_2$, 0 °C, KI;
(ii) aqueous NaOH (1M) in THF/MeOH, 30 min

Scheme 1

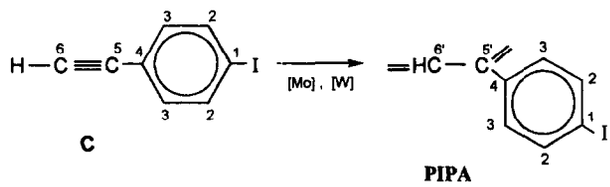

Scheme 2

induced by single $WOCl_4$ or $MoCl_5$ catalysts were simply started by mixing the solution of **C** (114 mg, 0.5 mmol) dissolved in benzene (2 ml) with the respective catalyst solution (1 ml, conc. 10 mmol l^{-1}). If a cocatalyst (Ph_4Sn or *n*-Bu_4Sn) was used, the catalyst solution (1 ml, conc. 10 mmol l^{-1}) was mixed with an equimolar (Mo-based catalyst) or twice that (W-based catalyst) amount of the cocatalyst (see *Table 1*) dissolved in benzene (0.5 ml), the mixture was allowed to ripen for 15 min and then mixed with the monomer (114 mg, 0.5 mmol in 1.5 ml benzene). If dioxane (1.5 ml) cosolvent was used, it was added to the ripe $WOCl_4/2Ph_4Sn$ catalyst system (15 min in 1.5 ml benzene) and, after 15 min, the resulting mixture was mixed with monomer **C** (114 mg, 0.5 mmol) dissolved in *ca.* 0.2 ml of solvents distilled from the catalyst mixture. The polymerization was always quenched by pouring the reaction mixture (3 ml) into 15 ml methanol. The methanol-insoluble polymer was filtered off, washed with methanol and dried in vacuum to the constant weight. The yield of the polymer was determined gravimetrically. The supernatant from the polymer isolation was analysed by g.c.-.m.s. in order that the total conversion of **C** be determined by the calibration curve method. The prepared poly(*p*-iodophenylacetylene) (PIPA) samples were stored in sealed, evacuated ampoules.

The kinetics of PIPA degradation in solution was measured as the time decrease in the degree of polymerization of the polymer[12–15]. Series of s.e.c. analyses of the polymer solution in THF (conc. 0.05 mg ml^{-1}) permanently exposed to air at room temperature was performed and the degradation rate constant, v, was obtained by evaluating the results according to equations (1) and (2) (ref. 33).

$$1/\langle X\rangle_n = 1/\langle X\rangle_{n,0} + \nu t \quad (1)$$

$$1/\langle X\rangle_w = 1/\langle X\rangle_{w,0} + \int_0^t (\nu/3) I_w \, dt \quad (2)$$

where t is the time of degradation, $\langle X\rangle_n$, $\langle X\rangle_w$ and $\langle X\rangle_z$ the number-, weight- and z-average degree of polymerization, respectively, and $I_w = \langle X\rangle_z/\langle X\rangle_w$ is the index of polydispersity based on the weight distribution of X. In the case that the polymer under degradation has achieved the most probable (Schulz–Flory) distribution of X, $I_w = 3/2$ and the integral variable on the right-hand side of equation (2) is equal to $(\nu/2)t$.

Electrical and photoelectrical measurements

Sample preparation. The measurements were performed on thin polymer films prepared under argon atmosphere by spin casting on stainless steel discs. The films of PIPA were cast from dioxane solutions whereas those of PPA from toluene solutions. The film thickness, being controlled by the spinning rate and the solution concentration, was varied from 1 to 5 μm in order that the thickness of the film surface layer (in which the charge carriers are generated) would be very low or negligible in comparison with the total film thickness. The films were dried under argon overnight and then in

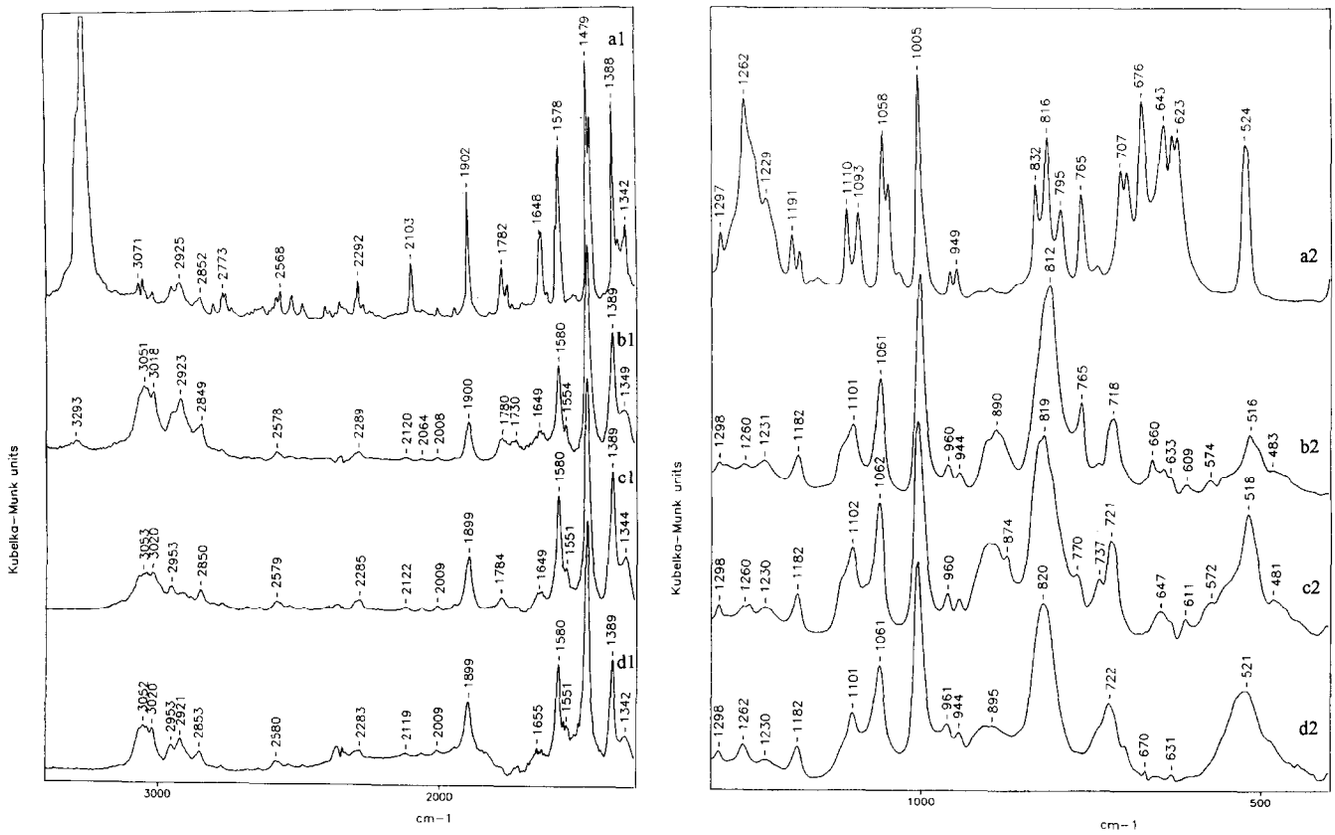

Figure 1 Diffuse reflectance i.r. spectra of monomer **C** (a1, a2) and of PIPA prepared with the $MoCl_5$ (b1, b2), $WOCl_4/2Ph_4Sn/Diox$ (c1, c2), and $WOCl_4/2Ph_4Sn$ (d1, d2) catalysts

vacuum (rotary pump, pressure 10 Pa) at a temperature of 320 K for 6 h to obtain homogeneous, crush-less films.

Quantum efficiency of the charge carrier photogeneration, η, was measured by the xerographic discharge method[34] using an instrument with a time resolution of 20 ms. The surface potential was measured with a rotary electrodynamic condenser electrometer[35]. In each measurement cycle, the surface of the polymer film was first charged in the dark using a corona discharge and, after some time, it was illuminated by a steady light source. The light exposures were derived from a UV-CAMAG lamp using band filters for wavelengths, λ, 254 nm and 366 nm, which are close to the absorption maxima of the polymers. The emission-limited conditions (under which the photoinduced quantum efficiency is independent of both the sample thickness and light intensity[34]) were achieved by an appropriately low radiation intensity used during the measurements of 2×10^{17} photons $m^{-2} s^{-1}$ and 1×10^{18} photons $m^{-2} s^{-1}$ for 254 nm and 366 nm illumination, respectively. The light penetration depth was about 100 nm (i.e., at least 10 times lower than the film thickness). No dependence of measured values of η on the light intensity and sample thickness was observed under these conditions. The surface potential decay was monitored both in the dark and under illumination and the values of η were obtained in a standard way using

$$\eta = [(\varepsilon_0 \varepsilon_r)/(e\Phi L)] (dU/dt)_{t=t0} \quad (3)$$

where ε_0 and ε_r are the absolute and relative permittivity of the polymer, respectively, e the unit charge, L the film thickness, Φ the absorbed photon flux and $(dU/dt)_{t=t0}$ the rate of the surface potential decay at the onset of illumination. The values of η were corrected to the dark surface potential decay from which the dark conductivity of the polymer sample was also estimated. To minimize an influence of trapped space charges and to achieve a better reproducibility of measured values, the sample was always allowed to discharge down to the zero value of the surface potential and to relax in the dark between measuring cycles.

RESULTS AND DISCUSSION

*Polymerization of (*p*-iodophenyl)acetylene*

The polymerization data are summarized in *Table 1*. First, it is seen that high degrees of the monomer conversion (mostly >90%) were achieved with both types of catalyst applied. Second, the $MoCl_5$-based catalysts provided relatively low yields of dark red insoluble PIPA (10–25%), whereas the $WOCl_4$-based catalysts provided rather high yields of red, soluble PIPA (50–90%). The differences found between the monomer conversion and the polymer yield are mainly due to the formation of oligomers observed in s.e.c. records of the supernatants from the polymer isolation. The $MoCl_5$-based catalysts provided considerably higher amounts of oligomers (*ca.* 60–85%) than the $WOCl_4$-based catalysts (10–45%). This finding corresponds with the literature data on the polymerization of phenylacetylene (PhA) for which the W-based catalysts are reported to exhibit higher activity than the Mo-based ones[6,7]. It is, however, worth mentioning that, on the contrary, practically equal polymer yields are reported for polymerizations of (bromophenyl)acetylenes induced by Mo- and W-based catalysts[37].

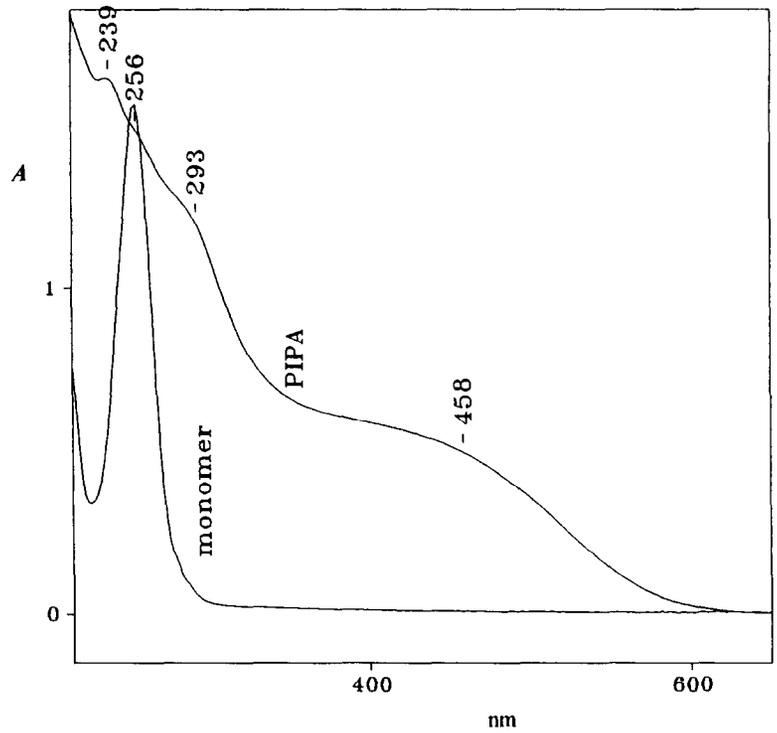

Figure 2 U.v.-vis spectra of monomer **C** and PIPA prepared with $WOCl_4/2Ph_4Sn$/Diox catalyst (sample No. 6b); THF, conc. 0.025 mg ml^{-1}

As far as the cocatalyst effect is concerned, surprisingly, an addition of both tested organotin cocatalysts has resulted in a decrease in the PIPA yield attained in benzene (*Table 1*, experiments No. 2, 3 and 5) although both the cocatalysts are known to increase polymerization efficiency of $MoCl_5$ and $WOCl_4$. This is even in the case of the $WOCl_4/Ph_4Sn$ catalyst system for which the optimum molar composition 1/2 is given, based on its activity in polymerization of phenylacetylene[38,39]. On the other hand, the addition of dioxane to the $WOCl_4/2Ph_4Sn$ catalyst system (experiment No. 6) has resulted in a considerable suppression of oligomer formation (below 10%) and in an increase in both the yield and molecular weight of PIPA. The effect of dioxane observed here is at least comparable with the effect observed in polymerization of phenylacetylene with the $WOCl_4/2Ph_4Sn$ catalyst system[14]. This effect can be attributed to a reversible coordination of dioxane molecules to the growing species which hinders their termination and makes the oligomer formation difficult. The observed formation of a stable complex of the composition $2WOCl_4$.dioxane[40] strongly supports this explanation.

*Characterization of poly(*p*-iodophenylacetylene)s*

Samples of PIPA prepared on the $WOCl_4$- and $MoCl_5$-based catalysts differ substantially in the solubility. The former are soluble in THF and dioxane while the latter are insoluble in both the last and in other solvents tested as well (aromatics, dimethyl sulfoxide, 1,2-dichloroethane, chloroform). The suspicion that the PIPA prepared with $MoCl_5$-based catalysts is insoluble due to its crystallinity was examined by low-angle X-ray diffraction analysis of the polymer. The diffraction pattern showed only broad reflection band at $2\Theta = 20°$ which corresponds to the most probable distance of the structure units in the amorphous phase. The crystallinity can be thus excluded as a reason for the polymer insolubility.

It is worth mentioning that PIPA always precipitates from the reaction mixture during the polymerization of **C** in benzene. In the benzene/dioxane mixture (1/1 by vol.), significant amounts of PIPA remain dissolved in the reaction mixture. Utilizing this effect, PIPA was split into two fractions (see *Table 1*) which were both soluble in THF. The determined values of molecular weight averages and low values of polydispersity indices of both the fractions prove that PIPA was fractionated according to the molecular weight. Besides crosslinking, too high molecular weight might thus be regarded as a possible reason for the observed insolubility of PIPA prepared with Mo-based catalysts.

^1H n.m.r. spectrum of soluble PIPA (prepared with $WOCl_4$ single component catalyst) measured in $CDCl_3$ consists of two partly overlapped broad bands of comparable intensity with δ ranging from 5.2 to *ca.* 7.0 ppm and *ca.* 7.0–8.0 ppm. The former should be attributed to overlapped signals of olefinic proton H6′ and a part of aromatic protons (H3?) and the latter to the signals of aromatic protons (H2?).*^{13}C n.m.r.* spectrum of PIPA prepared with $WOCl_4$ measured in $CDCl_3$ solution consists of the following bands: *ca.* 132–142 ppm (broad band of quaternary carbons, C4 and C5′); 136–138 ppm (C2) and 126–132 ppm (C3 and C6′); 93–94 ppm (C1). The assignment was made on the basis of APT (Attached Proton Test) spectrum of PIPA and the spectrum of monomer. No significant difference in the *solid state* *^{13}C n.m.r.* spectra of the PIPA samples prepared with $WOCl_4$ and $MoCl_5$ single component catalysts was observed. Both spectra consist of the signal of C1 carbon at 94 ppm and the broad band of the other carbons lying between 120 and 150 ppm (with two maxima at 137.5 and 130 ppm). Insufficient resolution of the n.m.r. spectra did not allow us to draw reliable information on the configurational structure of the studied PIPA samples.

The diffuse reflectance *i.r.. spectra* of **C** and the PIPA

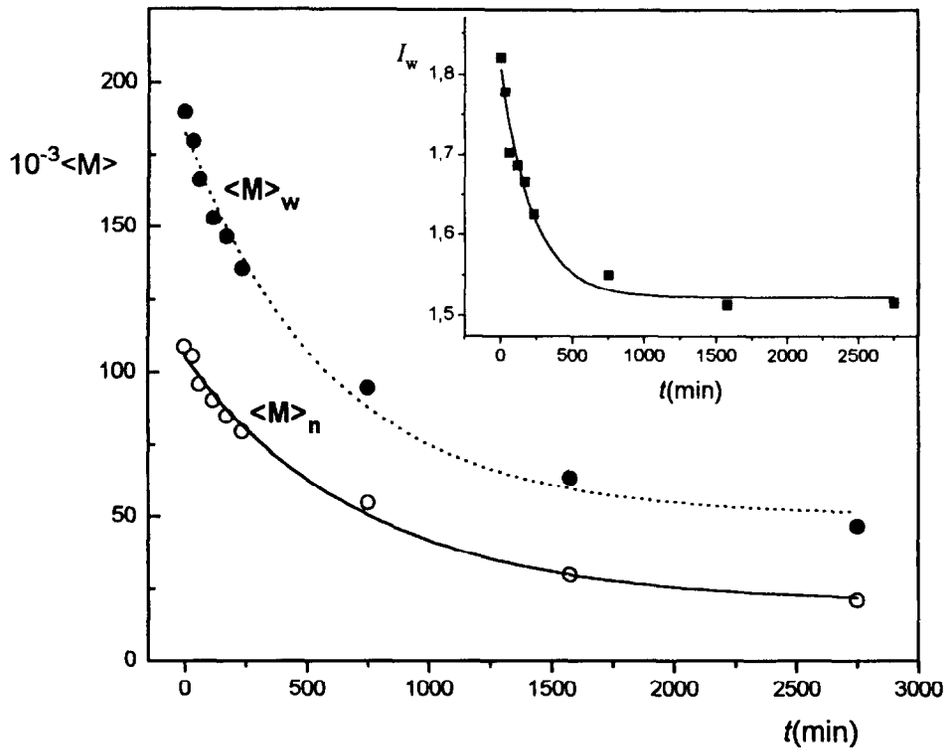

Figure 3 Time dependence of the number-average, $\langle M \rangle_n$, and weight-average, $\langle M \rangle_w$, molecular weight and polydispersity index (based on weight distribution), I_w, of PIPA (sample No. 6b) in the course of degradation in THF solution in air at 25°C

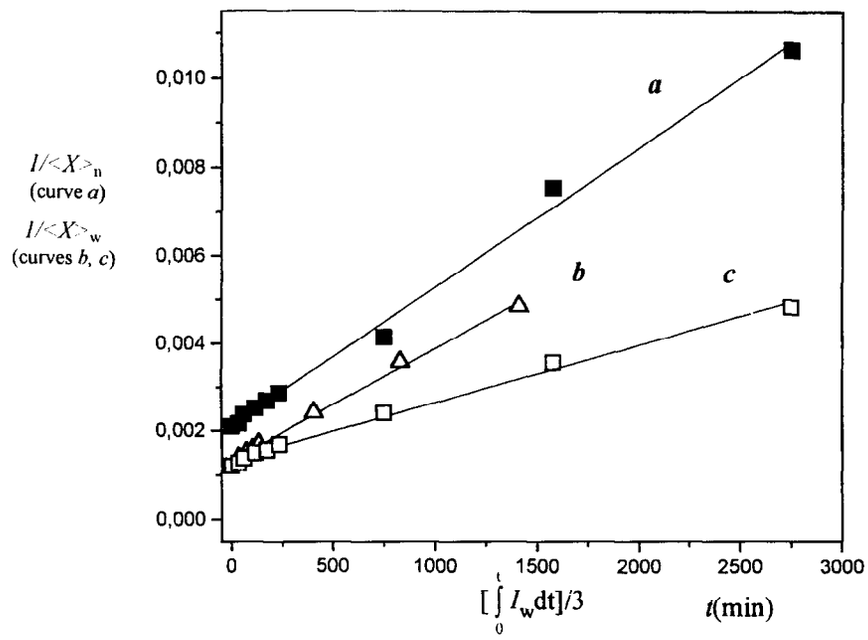

Figure 4 Plots of dependences obtained from the evaluation of experimental data on the PIPA degradation according to equation (1) (curve *a*) and equation (2) (exact formula, curve *b*; simplified formula, curve *c*)

samples prepared with the use of $MoCl_5$, $WOCl_4/2Ph_4Sn$ and $WOCl_4/2Ph_4Sn$/Diox catalysts, respectively, are shown in *Figure 1*. The transformation of **C** into polymer is evidenced in the i.r. spectra of polymers by: (a) the absence of bands characteristic of triple bonds: 3268(*vs*) cm^{-1} $\nu(\equiv C-H)$, 2103(*m*) cm^{-1} $\nu(C\equiv C)$, 1262(*s*) cm^{-1} $\nu(C-C\equiv)$, some of bands from 623(*m*) cm^{-1} to 676(*m*) cm^{-1} $\delta(H-C\equiv C)$; and (b) the presence of new bands (compared to the monomer spectrum) attributable to the vibrational modes of conjugated double bonds: 720(*m*, *b*) cm^{-1} $\delta(C=C-H)$, 890(*m*, *b*) cm^{-1} $\delta(C=C-H)$. Also the shoulders at 1555(*vw*) cm^{-1} and broad bands at 1640 cm^{-1} are attributable to $\nu(C=C)$ modes in conjugated systems[41–44].

The spectra of PIPA prepared with different catalyst systems are closely related to each other. Nevertheless, differences in $\delta(C=C-H)$ modes are seen in the regions about 650 cm^{-1}, 720–770 cm^{-1} and 850–900 cm^{-1} which testify to differences in the double-bond configurational structure of particular

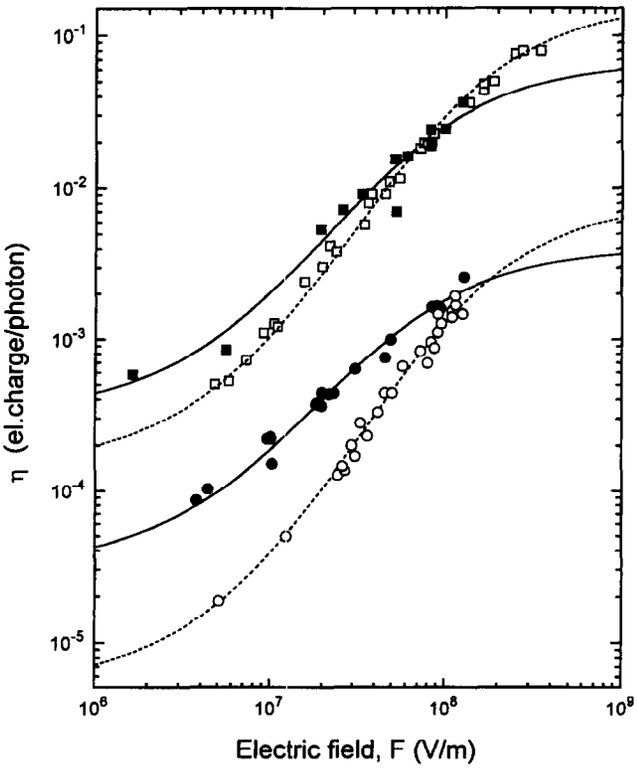

Figure 5 The dependence of the quantum photogeneration efficiency, η, on the applied electrical field, F, for positively charged samples at given excitation wavelength and room temperature: ■, PIPA, 254 nm; ●, PIPA, 366 nm; □, PPA, 254 nm; ○, PPA, 366 nm. Curves calculated according to the Onsager model

samples. Remarkable differences are also seen in the band at 525 cm^{-1} which should be ascribed to substituent-sensitive vibrations of phenyl rings. It is thus certain that the studied PIPA samples differ relevantly in the configurational structure. However, an assignment of the differences to particular structures can be made only tentatively, rather on the basis of reported correlation between the catalyst type and the polymer configurational structure. The Mo-based catalysts are known to produce high-*cis* whereas W-based catalysts high-*trans* poly(phenylacetylene)[43]. The addition of dioxane to the $WOCl_4/2Ph_4Sn$ catalyst system was found to increase the *cis* structure content in poly(phenylacetylene)[14]. Thus we can only tentatively assign the structures of studied PIPA samples prepared with different catalysts in the following way: $MoCl_5$-based (high-*cis*); $WOCl_4/2Ph_4Sn$/Diox (medium-*cis*); $WOCl_4/2Ph_4Sn$ (high-*trans*).

The *u.v./vis spectra* of monomer **C** and high-molecular-weight PIPA prepared with $WOCl_4/2Ph_4Sn$/Diox catalyst are shown in *Figure 2*. The PIPA spectrum consists of broad band with continuously decreasing absorption extended to the visible region (up to about 600 nm) which is due to the presence of long conjugated sequences in the polymer.

*Autoxidative degradation of poly(*p*-iodophenylacetylene) in THF solution*

The instability of polymers of monosubstituted acetylenes is well known[1,7,13,15,19]. Because the films for measurements of photoelectrical properties are usually prepared by casting from solutions, it is important to know the stability of particular polymer in solution under the atmospheric conditions. The degradation experiments were carried out as described in the Experimental section. It is notable that measurement of time decrease in the polymer molecular weight is perhaps the most sensitive method for monitoring the polymer degradation because it allows us to detect almost negligible degrees of conversion achieved in this reaction. Let us, for example, consider a polymer of the initial value of $\langle X \rangle_n$ equal to 1000, which possesses two equally reactive links per one monomeric unit (a typical polymer formed by chain polymerization of an unsaturated monomer). A cleavage of only 0.05% of the polymer mainchain bonds (i.e. attainment of the degree of conversion of 0.0005) results in the 50% decrease in its $\langle X \rangle_n$ value. Such a pronounced change in $\langle X \rangle_n$ is easily detectable by s.e.c. although not measurable by the i.r. or n.m.r. methods.

The results of degradation experiments are shown in *Figures 3* and *4*. The former provides a classical presentation of PIPA degradation in terms of the time dependences of the number-average, $\langle M \rangle_n$, and weight-average, $\langle M \rangle_w$, molecular weights. In the inset of *Figure 3*, the time dependence of the polydispersity index I_w of high-molecular-weight PIPA (sample No. 6b) is also shown. According to the theory[33,45], the I_w vs t dependence should approach the value of 1.5 for sufficiently high values of time, t, if the polymer degradation is of the random type (this means that the probability of scission is the same for any main-chain bond). *Figure 4* shows the plots obtained from the evaluation of experimental data according to equations (1) and (2). The values of integral variable for the dependence according to equation (2) were obtained by the numerical integration of the I_w vs time dependence shown in *Figure 3*. Evaluation of the dependences provided the value of the rate constant ν equal to $2.6 \times 10^{-6}\,min^{-1}$ (this means that the rate constant of a main-chain bond decay is $1.3 \times 10^{-6}\,min^{-1}$ because each monomeric unit contributes to the main chain by two bonds). For unsubstituted PPA prepared in the same way as the measured PIPA sample ($WOCl_4/Ph_4Sn$/Diox system), a slightly lower value of the rate constant ($\nu = 2.0 \times 10^{-6}\,min^{-1}$) was found[15]. It thus seems that the introduction of an iodine atom to the *para* position of the phenyl ring slightly lowers the stability of macromolecules in THF solution exposed to air.

*Electrical and photoelectrical properties of poly(*p*-iodophenylacetylene)*

The values of photogeneration efficiency of free charge carriers, η, as obtained from the xerographic measurements on PIPA were found to be sensitive to the polarity of the applied electric field and to the excitation light wavelength. For positively charged samples the values of η are about ten times higher than for those charged negatively. This result shows that in PIPA, the holes are the majority charge carriers being more mobile than the photogenerated electrons.

The dependences of η on the applied electric field, F, for excitation wavelengths $\lambda_{ex} = 254$ nm and 366 nm are shown in *Figure 5* for both polymers (PIPA and PPA). It is seen that the η values for PIPA are slightly lower at the high-electric-field limit, and significantly higher in the region of lower and moderate electric fields as compared to PPA, the difference being more pronounced for longer excitation wavelength.

Table 2 The parameters of the free charge carriers photogeneration of in PIPA and PPA for excitation wavelength 254 and 366 nm as calculated according to the Onsager model (see text)

		η_0 (electrons/photon)		α (nm)	
Polymer	λ_{ex}	254 nm	366 nm	254 nm	366 nm
PIPA		0.07	0.004	2.4	2.7
PPA		0.15	0.009	1.7	1.6

The course of the η vs F dependences together with the observed increase in the η values towards shorter excitation wavelengths suggest that the photogeneration of charge carriers in PIPA can be described by the model consisting of: (a) photoexcitation of a molecule to a neutral excited state, (b) autoionization of the excited state resulting in a creation of a localized hole and quasi-free hot electron, (c) thermalization of the hot electron via fast inelastic scattering leading to a formation of Coulomb-field-bound geminate electron–hole pair usually referred to as the charge transfer (CT) state or CT pair, (d) electric-field-assisted thermal dissociation of CT pair into free carriers which is assumed to proceed according to the Onsager mechanism[46,47]. The fraction of absorbed photons converted to CT pairs, so-called primary quantum efficiency, η_0, is assumed to be independent of the electric field. The values of η_0 are equal to the high-electric-field limits of the η vs F dependences (cf. *Figure 5*). In disordered materials like polymers, it is reasonable to assume that the distances of charges in CT pairs, r, obey the Gaussian distribution $g(r) = N \exp(-r^2/\alpha^2)$ with normalization factor N and dispersion parameter α (the value of which is inversely proportional to the slope of the η vs F dependence at moderate electric fields). The data presented in *Figure 5* could be satisfactorily fitted by the theoretical equation based on the described model providing the values of parameters η_0 and α summarized in *Table 2*. Nevertheless, some uncertainty concerning the determined parameter values can arise due to the absence of experimental η data in the high electric-field-region because of the lower charge acceptance of film surface in corona charging during the xerographic experiments.

In terms of the described model, the fraction of absorbed photons converted to CT-pairs (which is represented by η_0) is lower, whereas the fraction of those converted to free charge carriers at low and moderate F (represented by corresponding η) is considerably higher in PIPA than in PPA. This means that in PIPA the dissociation of CT pairs to free charge carriers proceeds with higher efficiency. This corresponds with the found difference in values of α, since the Coulomb binding energy of CT pairs is inversely proportional to their charge-separation distance.

The dissociation of CT pairs into free charge carriers is the electric-field-assisted process. It thus seems reasonable to assume that not only external but also internal electric fields can take part in this process. It is notable that we have recently observed even more pronounced increase in the η value of PPA in the low- and moderate-electric-field regions upon the incorporation into PPA[48] (by means of copolymerization) of 6% of monomeric units bearing cobaltacarboranyl groups of zwitterionic character with dipole moment of 17.7×10^{-30} Cm (for the structure of comonomer see ref. 26). Therefore, contribution of the internal electric field of C–I dipoles (dipole moment of iodobenzene is 5.67×10^{-30} Cm) to the separation of CT pairs into free charge carriers can be suggested as a rational lying behind the observed increase in η at low and moderate electric fields upon the phenyl-ring iodination of PPA.

CONCLUSIONS

1-Ethynyl-4-iodobenzene (*p*-iodophenylacetylene), **C**, of high purity grade can be prepared in high yields from 1-amino-4-(trimethylsilylethynyl)benzene via diazotation substitution of amino group for iodine followed by elimination of $Si(CH_3)_3$ group.

Monomer **C** can be polymerized by $WOCl_4$-based metathesis catalysts providing high yields of soluble polymers (tentatively assigned as high-*trans*) of molecular weights up to 2×10^5. On the other hand, the $MoCl_5$-based catalysts provide lower yields of insoluble polymers of different configurational structure (probably high-*cis*) and, in addition, higher amounts of oligomers of **C**.

Homopolymer of **C**, PIPA, is unstable when exposed to air in solutions undergoing oxidative degradation like unsubstituted poly(phenylacetylene) (PPA). From the kinetic point of view, PIPA degradation in solution obeys the laws characteristic of the random degradation (same as PPA). Under the same conditions, the value of the degradation rate constant of PIPA is higher than that of PPA which proves the negative effect of iodine in the *para* position on the polymer stability in air.

The introduction of iodine atoms into the *para* positions of the phenyl rings of PPA results in decrease in the primary quantum efficiency η_0 (i.e., the efficiency of generation of CT pairs) but in increase in the charge carrier photogeneration at low and moderate electric fields. Participation of the internal electric fields of C–I dipoles in the separation of CT pairs into free charge carriers can be suggested as a rational lying behind this effect of iodination of PPA. However, further investigation of photoelectrical properties of functionalized polyacetylenes is needed for a plausible explanation of the observed effect of aromatic substitution on the properties of PPA.

ACKNOWLEDGEMENTS

Financial support from EU Commission (PECO, supplementary contract ERBCIPDCT 940617) is gratefully acknowledged. The authors are indebted to Dr V. Hanuš (The J. Heyrovský Institute of Physical Chemistry, Academy of Sciences of the Czech Republic) for measuring the mass spectra, Dr I. Němec (Department of Inorganic Chemistry, Charles University) for measuring the i.r. spectra and Dr V. Blechta (Institute of Chemical Process Fundamentals, Academy of Sciences of the Czech Republic) for measuring the n.m.r. spectra.

REFERENCES

1. Chien, J. C. W., *Polyacetylene—Chemistry, Physics and Material Science*. Academic Press, New York, 1984.
2. Skotheim, T. A., ed., *Handbook of Conducting Polymers*. Marcel Dekker, Inc., New York, 1986.
3. Billingham, N. C. and Calvert, P. D., *Adv. Polym. Sci.*, 1989, **90**, 1.

4. Brédas, J. L. and Silbey, R., ed. *Conjugated Polymers*. Kluwer Academic Publishers, Dordrecht, 1991.
5. Kiess, G. H., ed. *Conjugated Conducting Polymers*. Springer Verlag, Berlin, 1992.
6. Masuda, T. and Higashimura, T., *Adv. Polym. Sci.*, 1987, **81**, 121.
7. Shirakawa, H., Masuda, T. and Takeda, K., in *The Chemistry of Triple-Bonded Functional Groups Supplement C2*. ed. S. Patai. Wiley, New York, 1994, p. 945.
8. Prasad, P. N. and Ulrich, D. R., ed. *Nonlinear Optical and Electroactive Polymers*. Plenum Press, New York, 1987.
9. Prasad, P. N., *Polymer*, 1991, **32**, 1746.
10. Neher, D., Wolf, A., Leclerc, M., Kaltbeitzel, A., Bubeck, C. and Wegner, G., *Synth. Met.*, 1990, **37**, 249.
11. LeMoigne, J., Hilberer A. and Strazielle, C., *Macromolecules*, 1992, **25**, 6705.
12. Sedláček, J., Vohlídal, J. and Grubišic-Gallot, Z., *Makromol. Chem. Rapid Commun.*, 1993, **14**, 51.
13. Vohlídal, J., Rédrová, D., Pacovská, M. and Sedláček, J., *Collect. Czech. Chem. Commun.*, 1993, **58**, 2651.
14. Sedláček, J., Pacovská, M., Vohlídal, J., Grubišic-Gallot, Z. and Žigon, M., *Macromol. Chem. Phys.*, 1995, **196**, 1705.
15. Vohlídal, J., Kabátek, Z., Pacovská, M., Sedláček, J. and Grubišic-Gallot, Z., *Collect. Czech. Chem. Commun.*, 1996, **61**, 120.
16. Kang, E. T., Ehrlich, P., Batt, A. P. and Anderson, W. A., *Appl. Phys. Lett.*, 1982, **41**, 1136.
17. Kang, E. T., Ehrlich, P., Batt, A. P. and Anderson, W. A., *Polym. Prepr.*, 1983, **24**, 73.
18. Pfleger, J., Nešpůrek, S. and Vohlídal, J., *Mol. Cryst. Liq. Cryst.*, 1989, **166**, 143.
19. Kang, E. T., Neoh, K. G., Masuda, T., Higashimura, T. and Yamamoto, M., *Polymer*, 1989, **30**, 1328.
20. Fujisaka, T., Suezaki, M., Koremoto, T., Inoue, T., Masuda, T. and Higashimura, T., *Polym. Prepr. Jpn*, 1989, **38**, 797.
21. Kmínek, I., Cimrová, V., Nešpůrek, S. and Vohlídal, J., *Makromol. Chem.*, 1989, **190**, 1025.
22. Tlenkopachev, M., Korshak, Y. V., Segizova, N. T., Bondarenko, G. N., Nechitailo, N. A. and Dzubina, M. A., *Vysomol. Soedin., A*, 1989, **31**, 1815.
23. Kalvoda, L., Kmínek, I., Cimrová, V., Nešpůrek, S., Schnabel, W. and Sedláček, J., *Colloid Polym. Sci.*, 1990, **268**, 1024.
24. Masuda, T., Abe, Y., Kouzai, H. and Higashimura, T., *Polym. J.*, 1994, **26**, 393.
25. Tlenkopachev, M., Korshak, Miranda, E. and Ogawa, T., *Polym. Bull.*, 1995, **34**, 405.
26. Vohlídal, J., Plešek, J., Sedláček, J., Císařová, I., Matějka, P. and Heřmánek, S., *Collect. Czech. Chem. Commun.*, 1996, **61**, 877.
27. Nešpůrek, S., Cimrová, V., Pfleger, J. and Kmínek, I., *Polym. Adv. Technol.*, 1996, **7**, 459.
28. Tamura, K., Masuda, T. and Higashimura, T., *Polym. J.*, 1985, **17**, 815.
29. Buchmeiser, M. and Schrock, R. R., *Macromolecules*, 1995, **28**, 6642.
30. Balogh, L. and Blumstein, A., *Macromolecules*, 1995, **28**, 5691.
31. Janevski, A., Leben, S., Šebenik, A. and Osredkar, U., *Synth. Met.*, 1992, **53**, 21.
32. Takahashi, S., Kuroyama, Y., Sonogashira, K. K. and Hagihara, N., *Synthesis*, 1980, 627.
33. Vohlídal, J., *Macromol. Rapid Commun.*, 1994, **15**, 765.
34. Chen, I., Mort, J. and Tabak, M. D., *IEEE Trans. Electron Devices ED-19*, 1972, 413.
35. Nešpůrek, S. and Ulbert, K., *Čs. Čas. Fyz.*, 1975, **25A**, 144.
36. Enck, R. G. and Pfister, G., in *Photoconductivity and Related Phenomena*, J. Mort and D. Pai, ed., Elsevier, Amsterdam, 1976.
37. Tlenkopachev, M., Korshak, Y. V., Segizova, N. T., Bondarenko, G. N., Nechitailo, N. A. and Dzubina, M. A., *Vysokomol. Soedin., B*, 1987, **28**, 55.
38. Vohlídal, J., Holander, A., Jančálková, M., Sedláček, J. and Sargánková, I., *Collect. Czech. Chem. Commun.*, 1991, **56**, 351.
39. Sedláček, J., Vohlídal, J., Kareš, J., Pacovská, M. and Máca, B., *Collect. Czech. Chem. Commun.*, 1994, **59**, 2455.
40. Fowles, G. W. A. and Frost, J. L., *J. Chem. Soc. A*, 1967, 671.
41. Socrates, G., *Infrared Characteristic Group Frequencies*. John Wiley, Chichester, 1980.
42. *SpecTool for Windows v. 1.1* (A Hypermedia Book for Structure Elucidation of Organic Compounds with Spectroscopic Methods), Chemical Concepts GmbH, Zurich, 1995.
43. Percec, V., *Polym. Bull.*, 1983, **10**, 1.
44. Horák, M. and Papoušek, D., *Infrared Spectra and the Structure of Molecules* (in Czech). Academia, Praha, 1976.
45. Simha, R., *J. Appl. Phys.*, 1941, **12**, 596.
46. Mozumder, A., *J. Chem. Phys.*, 1968, **48**, 1659.
47. Onsager, L., *Phys. Rev.*, 1938, **54**, 554.
48. Pfleger, J. and Vohlídal, J. Unpublished results.